



## Structural Damage Detection and Reliability Estimation using a Multidimensional Monitoring Approach

Journal:	<i>Part F: Journal of Rail and Rapid Transit</i>
Manuscript ID	JRRT-16-0118
Manuscript Type:	Article
Date Submitted by the Author:	05-May-2016
Complete List of Authors:	Ortiz, Juan ; Universidad EAFIT Escuela de Ingenieria, School of Mechanical Engineering Betancur Giraldo, German; Universidad EAFIT Escuela de Ingenieria, School of Engineering Gomez, Johnny; Universidad EAFIT Escuela de Ingenieria, School of Mechanical Engineering Castañeda, Leonel; Universidad EAFIT Escuela de Ingenieria, School of Mechanical Engineering Zajac, Grzegorz; Politechnika Krakowska im Tadeusza Kosciuszki, Mechanica Engineering Gutiérrez Carvajal, Ricardo Enrique; Universidad EAFIT Escuela de Ingenieria, School of Mechanical Engineering
Keywords:	RAMS, Railway Vehicle, Sensor Fusion, strain measurement, Superstructure
Abstract:	Many structural elements are exposed to load conditions that are difficult to model during the design stage, such as environmental uncertainties, random impacts and overloading amongst others, thus, increasing unprogrammed maintenance and reducing confidence in the reliability of the structure in question. One way to deal with this problem is to monitor the structural condition of the element. This approach requires supervising several signals coming from critical locations and then, performing an accurate condition estimation of the element based on the data collected. Herein, this paper implements a method to diagnosis and evaluate the reliability of the bolster beam structure of the railway-vehicle during a fatigue test. The results show that multidimensional monitoring not only provides an accurate diagnosis of the element, but also that this technique allows to estimate reliability correctly.


1  
2  
3  
4  
5  
6  
7  
8  
9  
10  
11  
12  
13  
14  
15  
16  
17  
18  
19  
20  
21  
22  
23  
24  
25  
26  
27  
28  
29  
30  
31  
32  
33  
34  
35  
36  
37  
38  
39  
40  
41  
42  
43  
44  
45  
46  
47  
48  
49  
50  
51  
52  
53  
54  
55  
56  
57  
58  
59  
60



SCHOLARONE™  
Manuscripts

For Peer Review

# Structural Damage Detection and Reliability Estimation using a Multidimensional Monitoring Approach

Journal Title  
XX(X):1–12  
© The Author(s) 2016  
Reprints and permission:  
sagepub.co.uk/journalsPermissions.nav  
DOI: 10.1177/ToBeAssigned  
www.sagepub.com/  


J. O. Ortiz<sup>1</sup>, German R. Betancur<sup>1</sup>, J. Gómez<sup>1,2</sup>, Leonel F. Castañeda<sup>1</sup>, G. Zajac<sup>3</sup> and R.E. Gutiérrez-Carvajal<sup>1</sup>

## Abstract

Many structural elements are exposed to load conditions that are difficult to model during the design stage, such as environmental uncertainties, random impacts and overloading amongst others, thus, increasing unprogrammed maintenance and reducing confidence in the reliability of the structure in question. One way to deal with this problem is to monitor the structural condition of the element. This approach requires supervising several signals coming from critical locations and then, performing an accurate condition estimation of the element based on the data collected. Herein, this paper implements a method to diagnosis and evaluate the reliability of the bolster beam structure of the railway-vehicle during a fatigue test. The results show that multidimensional monitoring not only provides an accurate diagnosis of the element, but also that this technique allows to estimate reliability correctly.

## Keywords

Structural Diagnosis; Structural Health Monitoring; Multidimensional Monitoring; Mechanical Systems; Singular Value Decomposition; Symptom Reliability.

## Introduction

Nowadays, structural health monitoring (SHM) is a topic of active research<sup>1</sup>. It consist of the entire process of signal acquisition, signal processing and computer decision support to plan maintenance activities of critical elements in order to increase reliability, availability, maintainability and security indexes (RAMS)<sup>2</sup>. SHM deals with real operational conditions, many of them difficult to model during the design stage, such as environmental effects, the alteration of load conditions during operation, structural fatigue and random impacts, amongst others<sup>3,4</sup>. This type of maintenance strategy allows one to estimate the best time to perform a maintenance task, thus providing for the availability of qualified operators, the suited tools for the task and so forth, overall improving the system to which the structure belongs<sup>5,6</sup>.

Railway-vehicles in particular, are designed to operate for at least thirty years, but real-life conditions present a complex mixture of

alternated loads specific to each railway system<sup>7</sup>, such as railway routes, type of vehicles, different operational schedules and maintenance programs amongst others. This could result in early wearing of components, such as cracks and fissures; requiring frequent corrective maintenance tasks and also dramatically reducing its life-time, in terms of operation and reliability<sup>8,9</sup>. These scenarios get worse if we take into account that the effort of SHM on railway-vehicle structures is limited to the bogie, leaving the maintenance program of the remaining elements mainly supported by non-destructive tests, avoiding real-time signal measurements that would otherwise

<sup>1</sup> Universidad EAFIT

<sup>2</sup> Instituto Tecnológico Metropolitano

<sup>3</sup> Cracow University of Technology

### Corresponding author:

R.E. Gutiérrez-Carvajal, GEMI research group Universidad EAFIT, Carrera 49 No. 7 Sur-50. Office 20-133, Medellín, Colombia.  
Tel: (57)(4)4489500 ext 9145.

Email: rgutier7@eafit.edu.co

1  
2  
3  
4  
5  
6  
7  
8  
9  
10  
11  
12  
13  
14  
15  
16  
17  
18  
19  
20  
21  
22  
23  
24  
25  
26  
27  
28  
29  
30  
31  
32  
33  
34  
35  
36  
37  
38  
39  
40  
41  
42  
43  
44  
45  
46  
47  
48  
49  
50  
51  
52  
53  
54  
55  
56  
57  
58  
59  
60

diagnose the structure inline<sup>10</sup>. One of these components is the bolster beam, which is the main structure of the carbody and is not a disposable piece. The diagnosis of a bolster beam consists of a set of non-destructive tests, such as those that include magnetic particles, ultrasound, permeable liquids, amongst others, that would require the whole train to be taken out of service, thus decreasing its availability. On the other hand, regarding fissures, the repair action would be to hire an expert operator to weld the fissure, whose level of expertise would depend on the location and type of weld<sup>11;12</sup>. Hence, it is critical for the maintenance manager to estimate when and where a fissure will appear.

Although there are several strategies for SHM reported in the literature<sup>13;14</sup>, such as the use of accelerometers and strain gauges measurements, acoustic signals, temperature sensors, machine vision and profile detectors, as far as we know, there have not been any applications of SHM to the bolster beam, despite the fact that this is a critical structure needed for vehicle operation, in which poor maintenance or incorrect loading can result in damage to both the infrastructure and passengers<sup>15</sup>. On the other hand, although full scale fatigue and fracture requires a huge invest of time and monetary cost, these studies play an important role in validating engineering designs. Notwithstanding the existence of analytical models and computational tools, this test provides the only reliable tool available to solve complex behaviours<sup>16</sup>.

Considering this issues, Universidad EAFIT designed and produced a new bolster beam element<sup>17</sup> to which we performed a destructive fatigue test, simulating extreme starts and stops with loads and thereafter conducting a health monitoring strategy based on multidimensional monitoring. It allows not only for a complete diagnosis of the system, but also to estimate the reliability of the element, highlighting the first region to fail.

Bearing these ideas in mind, the rest of the article is organized as follows: Materials and Methods explains the experimental setup and methods used; Results presents the results obtained with the proposed method, Discussion discusses the main results; and finally Conclusions introduces the main conclusions of this study.

## Materials and Methods

This study concerned to passenger vehicles similar in geometry and design to the ET420 trains set, e.g., Munich S-Bahn and Metro de Medellín<sup>18</sup>. In particular, the bolster beam is the structural element that supports the loads coming from the carbody and transmits to it to the bogie movement through the pivot at interface element, as is presented in Fig. 1. Universidad EAFIT designed a new bolster beam<sup>8;17</sup> and performed a fatigue test applying critical loads at the pivot, simulating impacts between bogie and the pivot, as reported by railroad operator.

### Experimental Set-up

A database of stress signal at fifteen points were constructed during a fatigue test of a bolster beam designed by Universidad EAFIT. In the following subsections, the experimental setup is explained in detail, firstly, introducing the product test laboratory of Universidad EAFIT and secondly, introducing the sensors placed at the element.

*Product Test Laboratory* The load test was performed using the Product Test Laboratory of Universidad EAFIT. It is made up of four systems, as demonstrated in Fig. 2:

1. Reaction structure. This supports the loads applied to the bolster beam. It consist of a reaction frame that allows the actuators to be placed in several configurations, a reaction wall and underframe, that permit the element of interest to be placed according to test protocol.
2. Power system. It is composed of the set of elements required to transmit loads to the test element, mainly a 6CTAA8.3-G1 Cummins<sup>®</sup> Motor, three Shore-Western<sup>®</sup> 922.5E actuators designed to apply 102 kN at tension and at 167 kN compression, two Shore-Western<sup>®</sup> 927E actuators designed to apply 995 kN and 1500 kN at tension and compression respectively<sup>19</sup>.
3. Control system. The power system is governed by a SC6000 controller system, an industrial computer running a software specifically designed for this purpose by the Shore Western<sup>®</sup> company<sup>20</sup>.
4. Monitoring system. The laboratory includes HBM<sup>®</sup> MGCPlus equipment configured

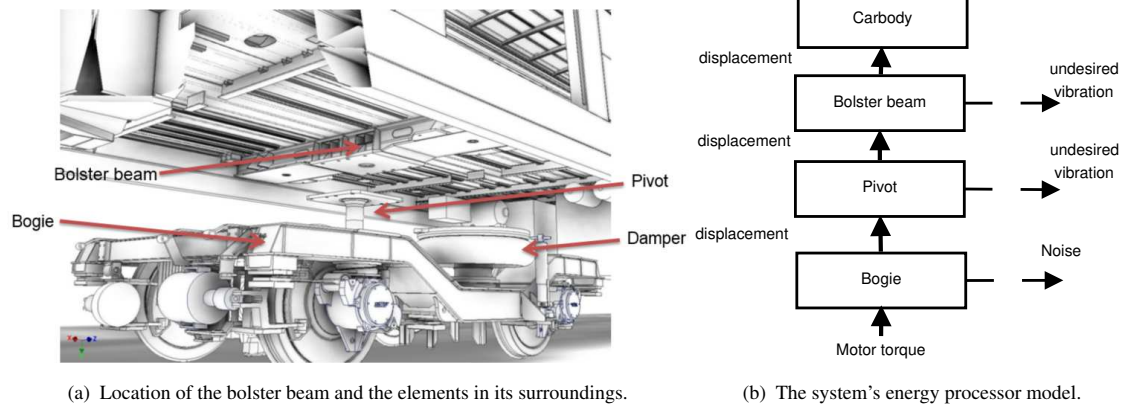


**Figure 1.** Railway-vehicle components. The bolster beam supports loads coming from the carbody and also from the bogie through the pivot as interface element.

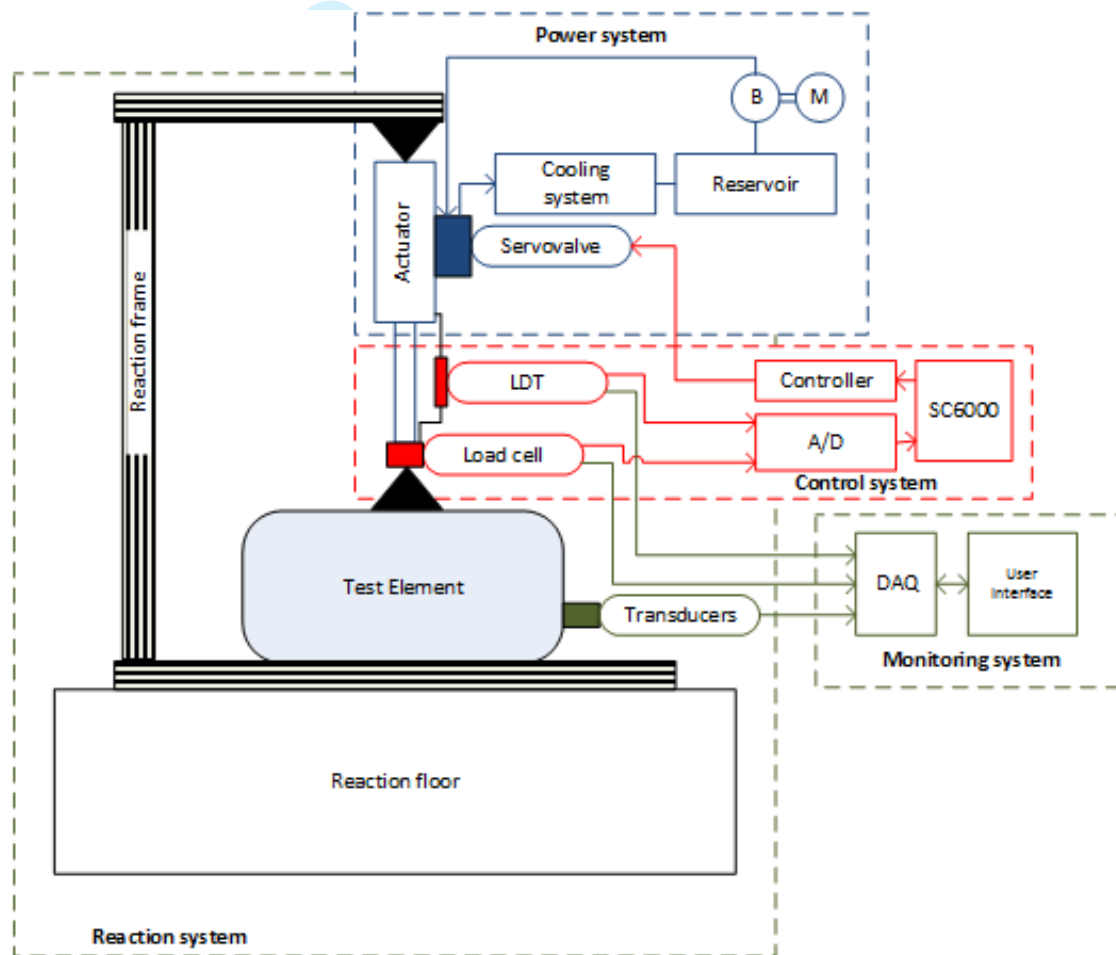


**Figure 2.** Diagram of conformation of the test laboratory at testing a particular element. There are four interacting systems: the reaction, power, control and monitoring systems.

with 5 AP815 cards devoted to dealing with strain gauges signals and two AP801S6 cards that acquire signals coming from accelerometer transducers.

*bolster beam Instrumentation* The bolster beam instrumented corresponds to the element patented in<sup>17</sup>. Three different types of sensors were located

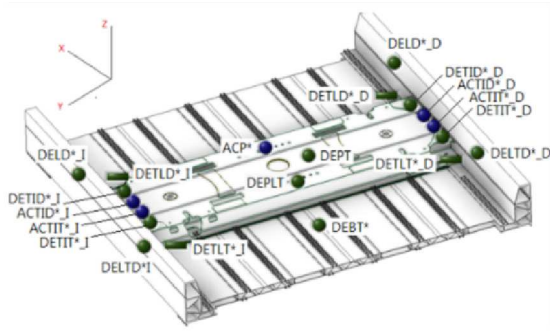


**Figure 3.** Location of sensors on the bolster beam.

along the bolster beam as presented in Fig 3, namely:

- Thirteen triaxial strain gauges (reference K-RY8-3-45-120-0), one located on the underframe of the structure (DEBT), and the rest symmetrically at the left and right sides of the bolster beam on the crossbars at the front and rear (DEL{D,T}), at the top surface of the bolster-beam, close to the weld that joins it with the crossbars at front and rear location (DETL{D,T}); at the frontal and rear surfaces of the bolster beam close to the welds that join it with the underframe (DETL{D,T});
- Two uniaxial strain gauges (reference HBW-35-125-6-3VR) located at the pivot of the bolster-beam, specifically placed to acquire signals from longitudinal (DEPLT) and transverse (DEPT) deformations;
- Three triaxial accelerometers (reference KISTLER<sup>®</sup> 8393 A K-BEAM), located at the top surface of the bolster beam on the front left side (ACTID\_I), rear right side (ACTIT\_D) and over the pivot (ACP);
- Two triaxial accelerometers (reference Brüel&Kjær<sup>®</sup> DeltaTron 4524), located on the top surface of the bolster beam at rear left side (ACTIT\_I) and the front right side (ACTID\_D).

### Methods

The method followed during this study consisted of analyzing data coming from a fatigue test performed over the bolster beam of a railway-vehicle. Strain signal was combined in each point of the analysis yielding to the current stress supported by the structure. Several indexes

of failure were extracted and several Symptom Observation Matrices (SOMs) were constructed for each point of analysis and then followed cycle by cycle.

This data is the result of the condition of the structural element after a certain number of cycles, allowing for decisions to be taken regarding elements that are currently placed in vehicles. The method overview is presented in Fig. 4. Firstly, stress signals from several different points were extracted from critical regions of the bolster. Secondly, those signals were preprocessed and thereafter transformed in stress estimations. Thirdly, several condition indexes were extracted and a SOM per signal was constructed. Finally, SOMs were used to perform diagnosis and prognosis of the structure.

**Fatigue Test** The fatigue test protocol consist of a sinusoidal load of 64.8 kN at the guide-rode gripper ( $F_{P_{1X}}$ ) at 1 Hz, simulating critical starts and stops of the bogie, and a load of 214.04 kN placed at the contact with the bogie limits ( $F_{P_{2X}}$ ) at 1 Hz in phase with  $F_{P_{1X}}$  due to the bodycar inertia when the vehicle is full loaded. Load locations and implementation is presented in Fig. 5.

Data coming from sensors were acquired at a sample rate of 300 Hz in parallel for all signals and stored using Catman<sup>®</sup> proprietary format using 61 channels including one pulse of synchronization between the SC6000 controller and the MGCPlus device. The test stopped after 3180 cycles when cracks at the pivot were evident.

**Signal processing and analysis** Before beginning the fatigue test one minute of signals was recorded in order to establish the value of each deformation without the signals being deformed from the pressure of loads. The average of each channel was subtracted from the signals acquired during the test. Principal stresses at critical regions in places where triaxial strain gauges were used were computed as in<sup>21</sup>. In the following equation, let  $E$  be the Young modulus,  $\nu$  the Poisson modulus,  $\epsilon_a$  the strain parallel to longitudinal loads,  $\epsilon_b$  the strain at 45° of the longitudinal loads and  $\epsilon_c$  the

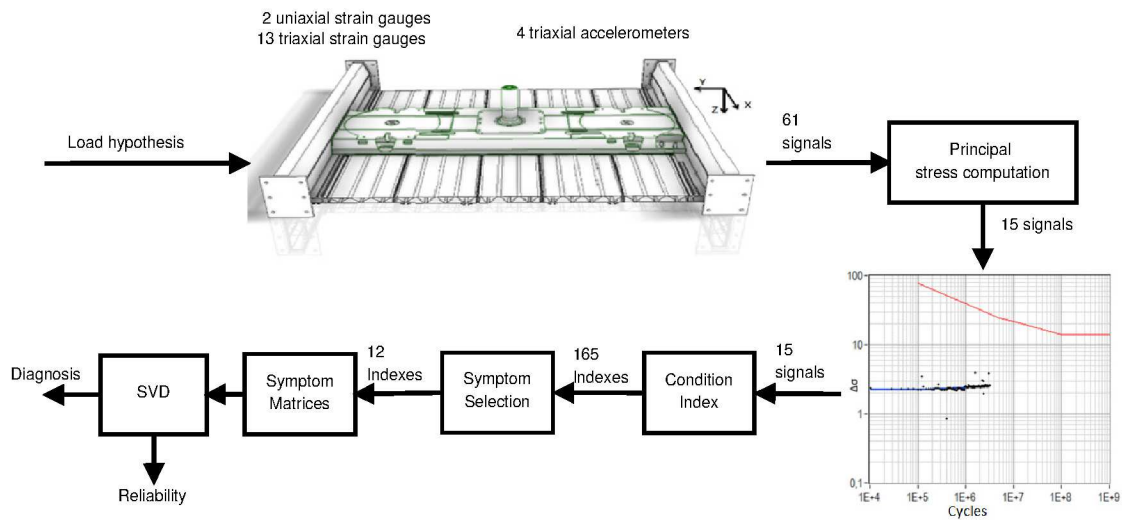


**Figure 4.** Method Overview. A fatigue test was performed evaluating extreme start and stop loads of the railway vehicle. Data coming from several sensors were recorded, preprocessed and analyzed to obtain stresses at critical places of the structure. Several indexes of condition were extracted and selected, reducing their redundancy. A SOM was thus constructed. Finally, structural diagnosis and its reliability across time were computed.

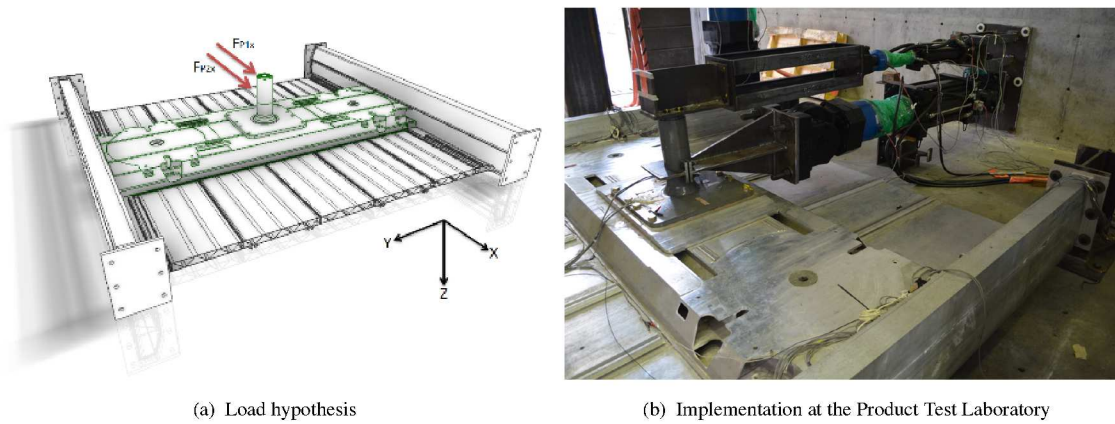


**Figure 5.** Configuration of Fatigue Test. Two loads were applied over the pivot simulating critical starts and stops: 1) road grid load over the pivot and 2) contact between pivot and the bogie longitudinal limits.

transverse strain:

$$\sigma = \frac{E}{1 - \nu} \frac{\epsilon_a + \epsilon_c}{2} + \frac{E}{\sqrt{2(1 + \nu)}} \sqrt{(\epsilon_a - \epsilon_b)^2 + (\epsilon_c - \epsilon_b)^2}. \quad (1)$$

Statistical moments of a one-second window were then extracted as descriptors of each stress signal, namely<sup>22</sup>: average ( $\mu$ ), standard deviation ( $std$ ), skewness ( $sk$ ), kurtosis ( $kurt$ ), root mean square ( $rms$ ), crest factor ( $cf$ ), and Fourier coefficients, as defined in Tab. 1.

*Symptoms selection* Notwithstanding, a huge number of signals taken does not mean that all

of them are significant to estimate the system's condition; signals coming from the element could present high redundancy, unnecessarily increasing the computational effort. To select meaningful symptoms, each symptom,  $S_i$ , was normalized by subtracting and dividing by its initial value,  $S_0$ , as suggested in<sup>23</sup>:

$$S_i = \frac{S_i}{S_0} - 1, \quad (2)$$

**Table 1.** Definition of Symptoms. Regarding the Fourier transform, only the coefficients that correspond to {0,1,2,3,4} Hz were used.

Symptom	Definition
Average ( $\mu$ )	$\mu = \frac{1}{N} \sum_{n=1}^N x_n$
Standard deviation ( $\sigma$ )	$\sigma = \sqrt{\frac{1}{N} \sum_{n=1}^N (x_n - \mu)^2}$
Skewness ( $sk$ )	$sk = \frac{\frac{1}{N} \sum_{n=1}^N (x_n - \mu)^3}{\left(\frac{1}{N} \sum_{n=1}^N (x_n - \mu)^2\right)^{3/2}}$
Kurtosis ( $kurt$ )	$kurt = \frac{\frac{1}{N} \sum_{n=1}^N (x_n - \mu)^4}{\left(\frac{1}{N} \sum_{n=1}^N (x_n - \mu)^2\right)^2} - 3$
Root Mean Square ( $rms$ )	$rms = \sqrt{\frac{1}{N} \sum_{n=1}^N x_n^2}$
Crest factor ( $cf$ )	$cf = \frac{ x _{peak}}{rms}$
Fourier transform amplitude ( $ \mathfrak{F}\{\mathbf{x}\} $ )	$\mathfrak{F}\{\mathbf{x}\}_k = \sum_{n=0}^N x_n e^{-\frac{2\pi}{N} kn}, j = \sqrt{-1}$

the dependency amongst symptoms  $s_i$  and  $s_j$  was then computed using the Pearson coefficient of correlation as:

$$r_{s_i, s_j} = \frac{\sum_{n=1}^N (S_{ni} - \mu_{s_i})(S_{nj} - \mu_{s_j})}{N \sigma_{s_i} \sigma_{s_j}}. \quad (3)$$

The most correlated symptom is selected as representative of all those symptoms that obtain correlations higher than a threshold of 0.6. A new subset of symptoms is created with the remain symptoms and the process is performed repeatedly until each symptom is represented.

**Multidimensional Condition Monitoring** Multidimensional condition monitoring is based on the holistic modeling<sup>24;25</sup>, representing the element as an open system using two resolutions of time: the high resolution one,  $t$ , in which the element has a particular signature in the signals coming from it, where the system is considered instantly time-invariant, and the life-time (low resolution)  $\theta$  which correspond to observations where the system could be considered time-variant; hence, if the system wears during operation, signals observed at time  $\theta_i$  must differ from others observed at  $\theta_j$ . It means that the system varies its efficiency over its life-time.

Herein, the symptoms matrix was constructed using the symptoms as columns of the SOM matrix

( $\mathcal{O}$ ) selected above, with each observation ( $\theta$ ) taken every 100 cycles, as in:

$$\mathcal{O}_{pr} = \begin{pmatrix} O_{\theta_1, S_1} & O_{\theta_1, S_2} & O_{\theta_1, S_3} & \cdots & O_{\theta_1, S_{12}} \\ O_{\theta_2, S_1} & O_{\theta_2, S_2} & O_{\theta_2, S_3} & \cdots & O_{\theta_2, S_{12}} \\ \vdots & \vdots & \vdots & \ddots & \vdots \\ O_{\theta_n, S_1} & O_{\theta_n, S_2} & O_{\theta_n, S_3} & \cdots & O_{\theta_n, S_{12}} \\ \vdots & \vdots & \vdots & \ddots & \vdots \\ O_{\theta_N, S_1} & O_{\theta_N, S_2} & O_{\theta_N, S_3} & \cdots & O_{\theta_N, S_{12}} \end{pmatrix}, \quad (4)$$

$N$  being the total number of observations. A way to decompose the SOM into linear combination of spaces is to perform a singular value decomposition (SVD)<sup>26;27</sup>, which allows for the generation of an index of failure ( $\Sigma$ ) w.r.t an orthonormal symptom space ( $\mathbf{U}$ ), formally:

$$\mathcal{O}_{pr} = \mathbf{U}_{pp} \Sigma_{pr} \mathbf{V}_{rr}^T, \quad (5)$$

$\mathbf{U}$  and  $\mathbf{V}^T$  are unitary matrices and  $\Sigma$  is a diagonal matrix composed of non-negative numbers. Thus, symptoms of damage (SD) were computed as:

$$\mathbf{SD}_i(\theta) = \Sigma_{ii} \mathbf{u}_i, \quad (6)$$

hence, the system damage at time-life  $\theta$  is computed as the sum of all symptoms of damage, formally:

$$\mathbf{SD}(\theta) = \sum_{i=1}^z |SD_i(\theta)| = \sum_{i=1}^z \Sigma_{ii} \cdot u_i(\theta). \quad (7)$$

Moreover, as  $\mathbf{U}$  is an orthonormal space, the diagonal of  $\Sigma$  governs the contribution of each vector to the symptom damage matrix, therefore, it is possible to use this information to construct



another index of general damage summing up the contribution of each vector as:

$$DS(\theta) = \sum_{i=1}^z |\Sigma_{ii}(\theta)|. \quad (8)$$

**Symptom Reliability** The holistic modeling approach suggests that there is a finite quantity of energy that the system could dissipate before it must get out of service, defining the energy of the system as the sum of the absolute value of the singular values<sup>28</sup>. It allows for the reinterpretation of the damage occurred during the lifetime of the element as the quotient between the current observed symptoms ( $\theta(S)$ ) and the limit allowed of the symptom in which the machine is not safe to work ( $\theta_l$ ):

$$D(S) = \frac{\theta(S)}{\theta_l(S)} \quad s.t. \quad \theta_l(S) > \theta(S). \quad (9)$$

Hence it is considered that the system will not continue in operation after reaching the limit  $\theta_l$  and hence  $0 < D(S) < 1$ . On the other hand, reliability ( $R$ ) is defined as the probability of a system to perform its task correctly, i.e., the system is operating below  $\theta_l(D)$ , hence, reliability is redefined as:

$$R(S) = 1 - \frac{\theta(S)}{\theta_b(S)} = 1 - D(S). \quad (10)$$

Typically, this limit is computed using a statistical test that measures the mean life of several elements with similar properties. However, in many cases it is not possible to get access to this information, due to a lack of specimens to test, a high variability in components and in the welding process itself (a huge number of specimens are indeed required). In this cases, it is preferable to adjust an *ad hoc* bound based on the reliability itself. Herein, we use the approach proposed in<sup>28</sup>, whose metric includes the desired availability  $P_g$  and the permissible probability of needless repair to avoid malfunctions:

$$R(S_l) = \frac{A}{P_g}, \quad (11)$$

the ratio  $A/P_g = 0.1$  representing the design rule<sup>28</sup>.

## Results

Table 2 introduce the symptoms selected by the redundancy reduction algorithm, based on the Pearson correlation coefficient. The symptoms are ranked according to their correlation with the remaining ones.

Figure 6 presents the generalized fault evolution. Figure 6(a) presents the evolution of the  $\|SD_i\|$ , which is equal to the singular value of the corresponding vector. The evolution of each generalized fault presents a monotonic behavior. The generalized fault profile  $DS$  evolution is introduced in Fig. 6(b), and is used as a measure of the overall condition of the system.

Figure 7 introduces the composition of the generalized failures  $SD_1$  and  $SD_2$ , being the most relevant in the construction of the overall condition estimator,  $DS$ . The contribution to each generalized fault was computed via the covariance matrix and normalized using its internal variability. In all cases, the main coefficient was related to the sensor closer to the location where a crack appeared and also in the direction of load application (DEPLT). The second most relevant coefficient was related to the sensor DETLD\_D, which is closer to the second weld that supports more stress in the bolster beam structure.

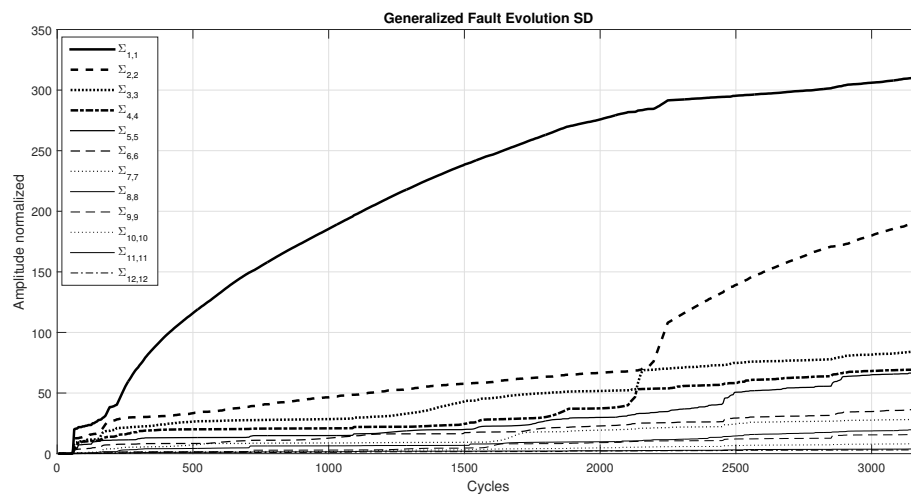
Figure 8 introduces the reliability symptom curve computed from the  $DS$  normalized by its first non-zero value. Using this curve and the reliability limit proposed above, the system could be safely used for a duration of 2000 cycles; after that, a maintenance task must be required. This result is coherent with the actual behavior of the couple pivot/bolster beam tested, as the pivot presented a crack after cycle number 2490.

## Discussion

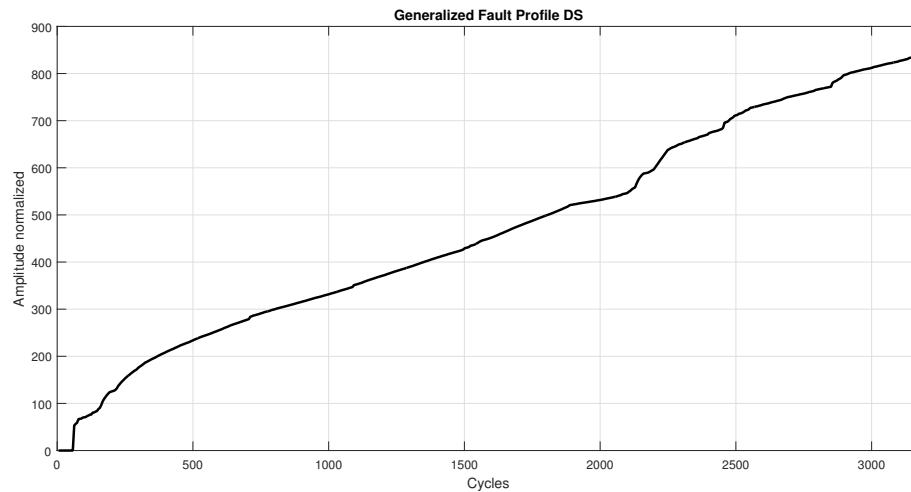
Structural monitoring deals with real conditions that are difficult to model during the design stage and also allows for the implementation of maintenance strategies for each specific device. This is a technique well suited for those structures that cannot withstand invasive or destructive tests. Also it is reported that continuously monitoring critical structures allows for a reduction in the cost of maintenance task, as the are addressed to the particular requirements of a specific structure, rather than a general policy based on periodic maintenance<sup>29</sup>.

**Table 2.** Symptoms selected after reduce their correlation. The closest sensor to the failure is presented in bold.

Symptom Number	Sensor Location	Feature
1	DETLT_D	Fourier coefficient at 4 Hz
2	DETLT_D	Skewness
3	DEBT	Skewness
4	DETLT_D	Fourier coefficient at 0 Hz
5	DETLT_I	Root Mean Square
6	DETLT_D	Fourier coefficient at 4 Hz
7	DELD_D	Standard Deviation
8	<b>DEPLT</b>	<b>Fourier coefficient at 1 Hz</b>
9	DETIT_D	Kurtosis
10	DETLT_I	Kurtosis
11	DETLT_I	Crest Factor
12	DETID_D	Skewness

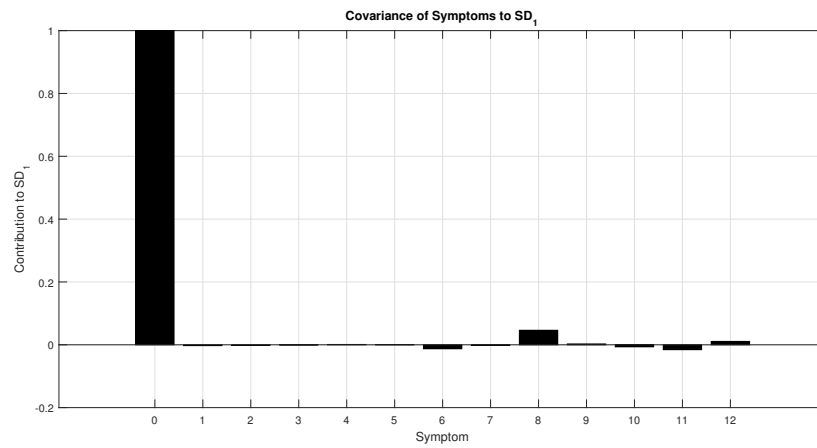


(a) Generalized Fault Evolution

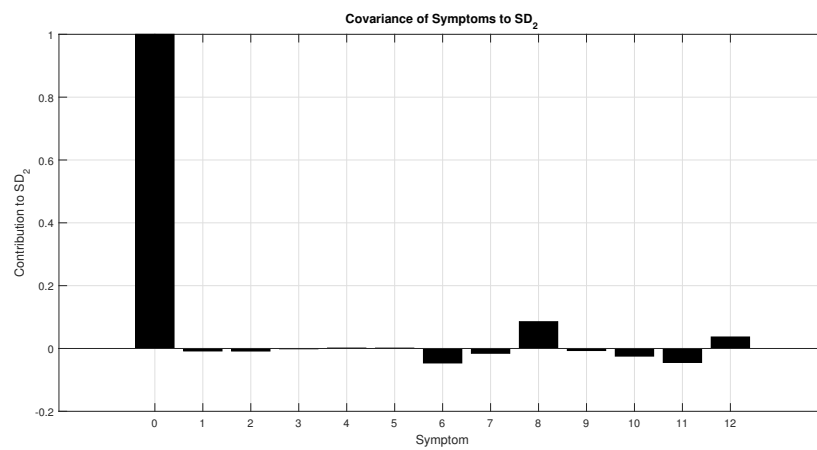


(b) Generalized Fault Profile

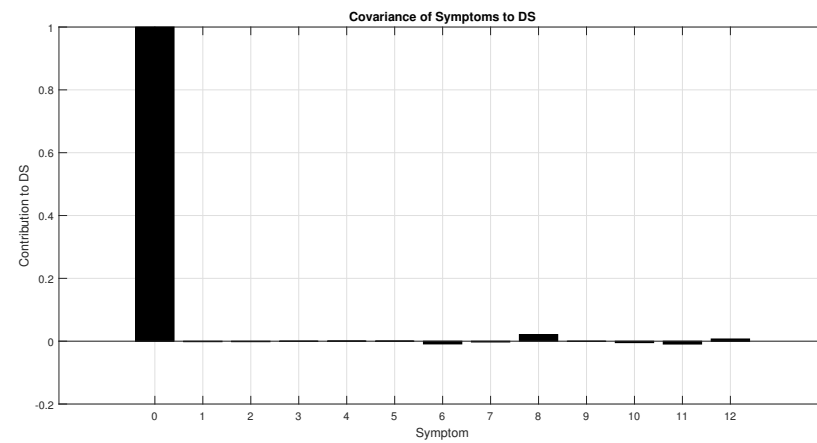
**Figure 6.** Generalized faults and generalized fault profile. Figure (a) presents the evolution of the energy of each generalized fault, i.e.,  $\Sigma_{ii}$ . In this case the first singular value rise faster than others. Figure (b) presents the generalized fault profile, it is the overall condition estimation, which is a monotonic rising function related to the overall system wear.



(a) Contribution of each symptom to  $SD_1$



(b) Contribution of each symptom to  $SD_2$



(c) Contribution of each symptom to DS

**Figure 7.** Contribution of symptoms to generalized faults, measured as covariance. The first covariance value is always one, as it is the autocovariance. Figures 7(a) and 7(b) presents the covariance of each selected symptom to the first two singular values. Figure 7(c) presents the covariance of each symptom to the generalized profile,  $DS$ . Note that in all cases the maximum covariance appears at sensor DEPLT, the sensor closest to the crack.

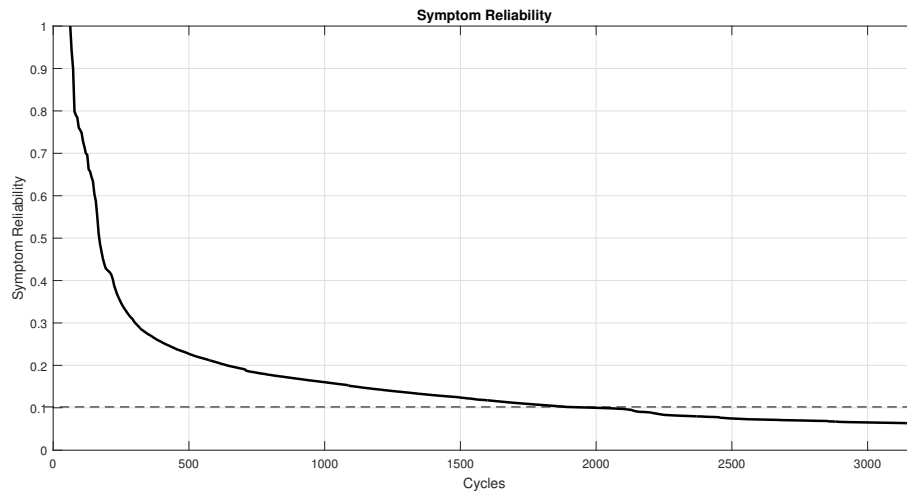


**Figure 8.** Symptom reliability. Accordingly to this graph, the system reaches 0.1 reliability after 2000 cycles of operation. The pivot of the bolster beam broke-down after 2490 cycles.

Currently, maintenance of the carbody structure is based on non-destructive tests, following a periodic inspection strategy. In this cases, the entire train is taken out of operation to perform the inspection, reducing its availability. Particularly, Schlake et al. recently proposed a method based on computer vision to identify fissures in the structure<sup>9</sup>. Despite the fact that it monitors the entire underframe structure, the failure must be visible by the naked eye and also, it does not directly instruct a maintenance task recommendation until it requires a corrective task to be undertaken. The method proposed herein to monitor the bolster beam not only estimates the current condition of the system, but also takes into account the history of the condition to construct a reliability function to guide the maintenance program.

Reliability is typically computed based on the time to the point of failure measured by a set of similar devices<sup>30</sup>. The inner variability in material composition, sensor sensitivity, low repeatability to perform welds and other such factors are all taken into account. The approach taken herein explodes the information coming from the history of a particular device and creates a specific reliability, reducing those uncertainties.

The method proposed differs from machine learning methods as they learns from examples, an action that limits the type of identifiable failures<sup>31;32</sup>. The proposed method estimate the

current reliability of the system based in several lowly-correlated symptoms and also finds the source of data that contributes the most to condition variation. Finally, the method explored in this article relates condition evolution with system reliability. Typically, to compute the reliability associated with a machine, it is necessary to measure the lifetime of a statistical significant number of similar devices<sup>33</sup>. On the contrary, the method used herein takes advantage of all the measurements performed in a particular system to the current reliability. It allows for a function to be fit over the reliability curve and predicts the best time to perform a maintenance task.

## Conclusions

This study presented the application of multidimensional monitoring to SHM, particularly concerning the bolster beam of a railway vehicle. The method is sensible to input signals, hence it was necessary to develop a strategy to reduce redundancy amongst symptoms, which consisted of a recursive algorithm based on the Pearson correlation coefficient. Multidimensional monitoring allowed for the combination of signals coming from several locations in the bolster beam and generated a single index to evaluate the entire system, which is directly related to its reliability. The technique not only recommended performing a maintenance task 490 cycles before the system

failed, but also accurately located the region of the failure.

## Acknowledgements

The authors want to acknowledge Universidad EAFIT staff for the support received to this study.

## Funding

This work was partially funding by the “Patrimonio autónomo Fondo Nacional de Financiamiento para la Ciencia, la Tecnología y la Innovación, Francisco José de Caldas”.

## Declaration of conflicting interests

The authors declare that there is not conflicting interests.

## References

- Seo J, Hu JW and Lee J. Summary review of structural health monitoring applications for highway bridges. *Journal of Performance of Constructed Facilities* 2015; DOI:10.1061/(ASCE)CF.1943-5509.0000824. URL [http://dx.doi.org/10.1061/\(ASCE\)CF.1943-5509.0000824](http://dx.doi.org/10.1061/(ASCE)CF.1943-5509.0000824).
- Farrar CR and Worden K. An introduction to structural health monitoring. *Philosophical Transactions of the Royal Society A* 2007; 365.
- Tlili L, Radhoui M and Chelbi A. Condition-based maintenance strategy for production systems generating environmental damage. *Mathematical Problems in Engineering* 2015; 2015: 12 pages. DOI:<http://dx.doi.org/10.1155/2015/494162>. URL <http://www.hindawi.com/journals/mpe/2015/494162/>.
- Lv Z, Wang J, Zhang G et al. Prognostics health management of condition-based maintenance for aircraft engine systems. *IEEE Conference on Prognostics and Health Management (PHM)* 2015; : 1–6 DOI:10.1109/ICPHM.2015.7245055.
- Gutiérrez-Carvajal RE, de Melo LF, Rosario JM et al. Condition-based diagnosis of mechatronic system using a fractional calculus approach. *International Journal of Systems Science* 2014; : 9 pages DOI:10.1080/00207721.2014.978833. URL <http://www.tandfonline.com/doi/full/10.1080/00207721.2014.978833>.
- Cho S. Probabilistic fatigue life prediction for bridges using system reliability analysis and shm-based finite element model updating. *12<sup>th</sup> International Conference on applications of Statistics and Probability in Civil Engineering* 2015; : 1–8.
- Martinod RM, Betancur GR, Osorio JF et al. A study of the effect of the transition curve in the coupling elements between the carbody and the bogie. *Transportation safety and security* 2014; 21(4): 351–363. DOI:<http://dx.doi.org/10.1504/IJHVS.2014.068113>.
- Aristizabal M, Barbosa JL, Betancur GR et al. Structural diagnosis of rail vehicles and method for redesign. *Diagnostyka* 2014; 15(3): 23–31.
- Schlake BW, Todorovic S, Edwards JR et al. Machine condition monitoring of heavy-axle load rail structural underframe components. *Proceedings of the Institution of Mechanical Engineers, Part F: Journal of Rail and Rapid Transit* 2010; .
- Ngigi RW, Pislaru C, Ball A et al. Modern techniques for condition monitoring of railway vehicle dynamics. *Journal of Physics: Conference Series* 2012; 364(1): 12–16. URL <http://stacks.iop.org/1742-6596/364/i=1/a=012016>.
- EN/ISO. EN/ISO 14731: Welding coordination tasks and responsibilities, 2006.
- EN/ISO. EN/ISO 14732:2013: Welding personnel - qualification testing of welding operators and weld setters for mechanized and automatic welding of metallic materials, 2013.
- Kouroussis G, Caucheteur C, Kinet D et al. Review of trackside monitoring solutions: From strain gages to optical fibre sensors. *Sensors* 2015; DOI:10.3390/s150820115.
- Liang JY and Deng XJ. *Structural Health Monitoring 2015: System Reliability for Verification and Implementation*, chapter Applications of Structural Health Monitoring on Intelligent High-speed Train. 2015. pp. 2037–2045.
- Barke D and Chiu WK. Structural health monitoring in the railway industry: a review. *Structural Health Monitoring* 2005; 4(1): 81–94. DOI:10.1177/1475921705049764. URL <http://shm.sagepub.com.ezproxy.eafit.edu.co/content/4/1/81.full.pdf+html>.
- Raghava G. Contribution to structural integrity: Fatigue and fracture related full scale experimental investigations carried out at csir-serc. *Procedia Engineering* 2014; 86: 139–149.
- Heredia LFC, Pérez JLB, Cano MA et al. Travesía para vehículos ferroviarios de pasajeros, procedimiento de ensamble de la misma y método para disponerla en un carrocería de vehículos ferroviarios, In process.
- Martinod RM, Betancur GR and Castañeda LF. Identification of the technical state of suspension elements in railway systems. *Vehicle System Dynamics* 2012; 50(7): 1121–1135. DOI:<http://dx.doi.org/10.1080/00423114.2012.656657>.
- Shore Western Manufacturing Inc., 225 W. Duarte rd. Monrovia, CA 91016. *User Manual 92XE Series Linear Actuators*, v20140728 ed, 2014.
- Shore Western Manufacturing Inc., 225 W. Duarte rd. Monrovia, CA 91016. *SC6000 Operation Guide v8.2.39, System Overview*, 2014.
- Hoffmann K. *An Introduction to Measurements using Strain Gages*. Hottinger Baldwin Messtechnik GmbH, Darmstadt, 1989.
- Martinod RM, Betancur GR, Castañeda LF et al. Estimation of combustion engine technical state by multidimensional analysis using svd method. *Vehicle Systems Modelling and Testing* 2013; 8(2): 105–118. DOI:<http://dx.doi.org/10.1504/IJVSMT.2013.054476>.
- Cempel C. Vibroacoustic condition monitoring. *NASA STI/Recon Technical Report A* 1991; 93.
- Natke HG and Cempel C. *Model-Aided Diagnosis of Mechanical Systems*. Springer, 1997.
- Natke HG and Cempel C. Holistic dynamics and subsystem modelling: principles. *International Journal of Systems Science* 1999; 30(3): 283–293.
- Cempel C and Tabaszewski M. Multidimensional condition monitoring of machines in nonstationary operation.

- 1  
2  
3  
4  
5  
6  
7  
8  
9  
10  
11  
12  
13  
14  
15  
16  
17  
18  
19  
20  
21  
22  
23  
24  
25  
26  
27  
28  
29  
30  
31  
32  
33  
34  
35  
36  
37  
38  
39  
40  
41  
42  
43  
44  
45  
46  
47  
48  
49  
50  
51  
52  
53  
54  
55  
56  
57  
58  
59  
60
- Mechanical systems and Signal Processing* 2007; 21(3): 1233–1241.
27. Cempel C. Decomposition of the symptom observation matrix and grey forecasting in vibration condition monitoring of machines. *International journal of applied mathematics and computer science* 2008; 18(4): 569–579.
28. Cempel C. Assessment of symptom limit value in vibration condition monitoring. *Proceedings of the First International Congress on Condition Monitoring and Diagnostic Engineering* 1989; : 29–33.
29. Ceravolo R, Pescarote M and Stefano AD. Symptom-based reliability and generalized repairing cost in monitored bridges. *Reliability Engineering & System Safety* 2009; 94(8): 1331–1339.
30. McPherson JW. *Reliability Physics and Engineering. Time-To-Failure Modeling*. New York, USA: Springer, 2010.
31. Mechbal N, Uribe JS and Rébillat M. A probabilistic multi-class classifier for structural health monitoring. *Mechanical Systems and Signal Processing* 2015; 60-61: 106–123.
32. Santos A, Figueiredo E, Silva M et al. Machine learning algorithms for damage detection: Kernel-based approaches. *Journal of Sound and Vibration* 2016; 363: 584–599.
33. Hasan Touama MB. Estimation and evaluation the reliability of production machines practical study of the textile department/the national establishment of the jordanian textiles in the industrial king abdullah ii city. *Procedia - Social and Behavioral Sciences* 2013; 93: 125–133.